ZEUS-prel-05-007-plus

Submitted to the
XXXIII International Conference on High Energy Physics
July 26 - August 2, 2006, Moscow, Russia

Abstract: **Session: QCDh, HQ**

Measurement of Charm Production Cross Sections and Fragmentation Fractions in Deep Inelastic Scattering at HERA

ZEUS Collaboration

Abstract

Charm production in deep inelastic scattering has been measured with the ZEUS detector at HERA using an integrated luminosity of approximately 80 pb^{-1}. Charm has been tagged by reconstructing $D^{*\pm}$, D^0, $D^\pm$, $D_s^\pm$ and $\Lambda_c^\pm$ charm hadrons. The kinematic region covered is $1.5\ \text{GeV}^2 < Q^2 < 1000\ \text{GeV}^2$, $0.02 < y < 0.7$. The charm hadrons have been measured in the kinematic range $p_T(D^{*\pm}, D^0, D^\pm, \Lambda_c^\pm) > 3$ GeV, $p_T(D_s^\pm) > 2$ GeV and $|\eta(D, \Lambda_c^\pm)| < 1.6$. The production cross sections are used for extracting the fractions of c quarks hadronising as a particular charm hadron in the kinematic range considered. The D^0, $D^\pm$ and $D_s^\pm$ cross sections are also compared with the predictions of next-to-leading-order QCD, and extrapolated to the full kinematic region in $p_T(D)$ and $\eta(D)$ in order to determine the open-charm contributions, $\text{F}_2^{c\bar{c}}(x, Q^2)$, to the proton structure function F_2.

1 Introduction

The HERA accelerator provides a variety of excellent means to test perturbative Quantum ChromoDynamics (pQCD) in depth. In particular, heavy quark production in ep interactions at the deep inelastic scattering (DIS) regime, is predicted to be largely dominated by the interaction, at the Born level, between the exchanged virtual boson (γ or Z^0) and a gluon within the proton; this is the so called Boson Gluon Fusion, BGF, mechanism. Heavy quark production provides a twofold test of QCD: the thorough study of the Born process and higher order corrections to the BGF reaction, and an independent check of the gluon density in the proton extracted from the NLO QCD analysis of the inclusive F_2 data, carried out with an exclusive reaction as heavy quark production.

Of the two heavy quarks whose production is accesible by HERA, c and b, the latter is strongly suppressed due to its smaller electric charge and larger mass. This paper studies c-quark production processes.

A charm quark in the final state is identified by the presence of a corresponding charmed hadron. This paper studies the production of those charmed particles to which the c-quark fragments with largest probability and with charged decay products which are accurately reconstructed by a detector such as ZEUS. These comprise the pseudo scalar mesons $D^0 \to K^-\pi^+$, $D^+ \to K^-\pi^+\pi^+$ and $D_s^+ \to \Phi\pi^+ \to K^+K^-\pi^+$, the vector meson $D^{*+} \to D^0\pi^+ \to K^-\pi^+\pi^+$ and the barion $\Lambda_c^+ \to pK^-\pi^+$ (unless explicitely stated the reference to a particle always indicates particle and antiparticle).

Since the D particle is measured and not the c-quark itself, the comparison with pQCD is indirect and requires a modelling of the c to D fragmentation. A consequence of the QCD factorization theorem [1] is that the "hard" (pQCD governed) c production mechanism is independent of the "soft" fragmentation process. Our measurements therefore give information about both, the features of the c-quark production which are common to all D particles produced, and the fragmentation of the c-quark to the different D particles measured.

This paper therefore has three aims: to measure c quark fragmentation properties, to test the universality of this fragmentation by comparing the results to the corresponding results from γp and e^+e reactions, and to test pQCD predictions for charm production. The data sample used was taken by the ZEUS detector during the years 1998 - 2000. The fragmentation measurements follow closely those reported recently by ZEUS in the photoproduction regime [2]. Using a variety of D mesons, the pQCD analysis complements the higher precision study done with D^* in the same data sample [3]. D^* measurements in this paper are used only for the extraction of the fragmentation parameters.

Other previous measurements of charm production in DIS with pQCD analyses [4–9] use mostly the D^* meson. There are also several measurements in the photoproduction regime [9–14]; here the much larger cross sections provide correspondingly better statistics, but in a more complicated initial state. Charm fragmentation studies in DIS done by the H1 experiment can be found in [15].

2 Experimental set-up

The data presented in this analysis were collected with the ZEUS detector at HERA during the 1998-2000 running periods, with $e^{\pm}$ beam energy of $E_e = 27.5$ GeV colliding with a proton beam energy of $E_p = 920$ GeV. The data sample corresponds to an integrated luminosity of 82 pb^{-1}.

A detailed description of the ZEUS detector can be found elsewhere [16]. A brief outline of the components that are most relevant for this analysis is given below.

Charged particles are tracked in the central tracking detector (CTD) [17], which operates in a magnetic field of 1.43 T provided by a thin superconducting solenoid. The CTD consists of 72 cylindrical drift chamber layers, organised in nine superlayers covering the polar-angle[1] region $15° < \theta < 164°$. The transverse-momentum resolution for full-length tracks is $\sigma(p_T)/p_T = 0.0058 p_T \oplus 0.0065 \oplus 0.0014/p_T$, with p_T in GeV.

The high-resolution uranium–scintillator calorimeter (CAL) [18] consists of three parts: the forward, the barrel and the rear calorimeters. The smallest subdivision of the calorimeter is called a cell. The CAL energy resolutions, as measured under test-beam conditions, are $\sigma(E)/E = 0.18/\sqrt{E}$ for electrons and $\sigma(E)/E = 0.35/\sqrt{E}$ for hadrons, with E in GeV.

3 Event selection

An event was selected if it satisfied the following criteria: a scattered electron was identified using a neural-network procedure [19] with energy $E'_e > 10$ GeV; $y_e \leq 0.95$; $y_{\rm JB} \geq 0.02$; $1.5 < Q^2_\Sigma < 1000$ GeV^2, where the subscripts e, JB and Σ refer to the electron, Jaquet-Blondel [20] and Σ- [21] methods, respectively; $40 < \delta < 65$ GeV, where $\delta = \sum_i (E - p_z)_i$ and the index i runs over a combination of tracks measured in CTD and CAL clusters; a reconstructed primary vertex with $|Z_{\rm vertex}| < 50$ cm is required; the

[1] The ZEUS coordinate system is a right-handed Cartesian system, with the Z axis pointing in the proton beam direction, referred to as the "forward direction", and the X axis pointing left towards the centre of HERA. The coordinate origin is at the nominal interaction point.

impact point (X, Y) for the scattered lepton in the RCAL must lie outside the region 26×14 cm^2 centred on $X = Y = 0$.

The measurements presented in this paper are corrected to the "true" kinematic region $1.5 < Q^2 < 1000$ GeV^2, $0.02 < y < 0.7$.

4 Reconstruction of charm hadrons

The reconstruction of D^0, D^+, D_s^+, D^{*+} mesons and Λ_c^+ baryons was performed in the kinematic region $p_T(D, \Lambda_c) > 3.0$ GeV and $|\eta(D, \Lambda_c)| < 1.6$. For pQCD comparisons and $F_2^{c\bar{c}}$ extrapolations, the $p_T(D_s^+)$ requirement was relaxed to $p_T(D_s^+) > 2$ GeV. This could be done because the constrain provided by the pair K^+, K^- coming from a ϕ meson keeps the combinatorial background still at acceptable levels.

The distributions were fitted assuming a "modified" Gaussian function, $\text{Gauss}^{\text{mod}} \propto \exp(-0.5x^{1+\frac{1}{1+0.5x}})$, where $x = |(M - M_{D,\Lambda_c})/\sigma|$, to describe the signal shape plus a background function. Only tracks measured in the CTD and fitted to the primary vertex were used in the reconstruction.

4.1 Reconstruction of D^0 mesons

The D^0 mesons were reconstructed from the decay channel $D^0 \to K^-\pi^+$ (+c.c.). In each event, D^0 candidates are formed from pairs of tracks with opposite charges and $p_T > 0.8$ GeV. A cut $|\cos\theta^*(K)| < 0.85$, where $\theta^*(K) = \text{angle}(\boldsymbol{p}_K^{(D^0 \text{ rest})}, \boldsymbol{p}_{D^0}^{(\text{lab})})$, was applied to reduce the contribution from combinatorial background. The D^0 candidates were separated in two groups. The "ΔM tag" group consists of D^0 candidates which are combined with a third track that could be a "soft" pion (π_s) in a $D^{*+} \to D^0\pi_s^+$ (+ c.c.) decay. The soft pion must have $p_T > 0.2$ GeV and charge opposite to that of the kaon. The cut value was $p_T > 0.25$ GeV for a data subsample, corresponding to an integrated luminosity of 17 pb^{-1}, for which the track reconstruction efficiency at low-momentum was smaller due to the operating conditions of the CTD [22]. For D^0 mesons not coming from a D^{*+}, the incorrect assignment of the pion and kaon masses to the two tracks produces a wider reflected signal. The reflected signal normalised to the ratio of numbers of D^0 without and with ΔM tag is subtracted from the untagged D^0 canditates. Figure 1 show the $M(K\pi)$ distribution for untagged D^0 candidates after the reflection subtraction (top) and tagged D^0 candidates (bottom), respectively. Clear signals are seen at the nominal value of $M(D^0)$. The number of D^0 untag (tag) mesons yielded by the fit was $N^{\text{untag}}(D^0) = 9910 \pm 940$ ($N^{\text{tag}}(D^0) = 1907 \pm 77$).

4.2 Reconstruction of "additional" D^{*+} mesons

The D^{*+} mesons were reconstructed from the decay channels $D^{*+} \rightarrow D^0 \pi_s^+$ (+c.c.) with $D^0 \rightarrow K^- \pi^+$ (+c.c.). The D^{*+} events within the D^{*+} kinematic range can be considered as the sum of events with D^0 tracks within the D^0 kinematic range (tagged D^0) plus events with D^0 tracks outside that kinematic range. The latter events correspond to additional D^{*+} mesons which were selected in the following way. In each event, pairs of tracks with $p_T > 0.4$ GeV were combined to form a D^0 candidate. Only combinations with invariant mass $1.80 < M(K\pi) < 1.92$ GeV were considered. These D^0 candidates lie outside the tagged D^0 kinematic range, i.e. they have $p_T(D^0) < 3.0$ GeV or $|\eta(D^0)| > 1.6$. A third track with $p_T > 0.2$ GeV ($p_T > 0.25$ GeV for the data subsample for which the track reconstruction efficiency at low-momentum was smaller) and charge opposite to that of the kaon track was combined with the D^0 candidate to form a D^{*+} candidate, and kept if its charge was opposite to the kaon track. Figure 2 shows the distribution of the mass difference $\Delta M = M(K\pi\pi_s) - M(K\pi)$ for these D^* candidates. A clear signal is seen around the nominal value of $M(D^{*+}) - M(D^0)$. The combinatorial background under the signal was estimated from the mass difference distribution of the wrong-charge combinations, in which both tracks associated to the D^0 candidate have the same charge and the third track has opposite charge. The number of reconstructed additional D^{*+} mesons was calculated by subtracting the wrong-charge ΔM distribution, after normalising it to the number of right-charge candidates in the region $0.150 < \Delta M < 0.165$ GeV. The subtraction was done in the signal region $0.143 < \Delta M < 0.148$ GeV and yielded $N^{\rm add}(D^{*+}) = 312 \pm 28$.

4.3 Reconstruction of D^+ mesons

The D^+ mesons were reconstructed from the decay channel $D^+ \rightarrow K^- \pi^+ \pi^+$ (+c.c.). Due to trigger availability, the D^+ sample corresponds to an integrated luminosity of 65 pb^{-1}. In each event, two tracks with the same charges and a third track with opposite charge were combined to form D^+ candidates. Tracks were required to have $p_T(\pi) > 0.5$ GeV and $p_T(K) > 0.7$ GeV. To reduce the combinatorial background, a cut in the variable $\cos\theta^*(K) > -0.75$ is imposed, where $\theta^*(K) = \mathrm{angle}(\boldsymbol{p}_K^{(D^+ \ \mathrm{rest})}, \boldsymbol{p}_{D^+}^{(\mathrm{lab})})$. To suppress background from D^{*+} and D_s^+ no combination with $M(K\pi\pi) - M(K\pi) < 0.150$ GeV and with $M(K^\pm$"$K^\mp$"$)$ within ± 8 MeV of the nominal ϕ mass was taken [10]. Figure 3 shows the $M(K\pi\pi)$ distributions for D^+ candidates. A clear signal is seen at the nominal value of $M(D^+)$. The number of D^+ mesons yielded by the fit was $N(D^+) = 3530 \pm 360$.

4.4 Reconstruction of D_s^+ mesons

The D_s^+ mesons were reconstructed from the decay channel $D_s^+ \to \phi\pi^+$ (+c.c.) with $\phi \to K^+K^-$. In each event, two tracks with opposite charges were combined to form the ϕ candidates whose invariant mass $M(KK)$ should be within ± 8 MeV of the nominal ϕ mass [10]. A third track was combined with the ϕ candidate yielding the D_s^+ candidate. Only tracks with $p_T(\pi) > 0.5$ GeV and $p_T(K) > 0.7$ GeV were considered. Combinatorial background was suppressed with the following cuts: $|\cos^3\theta^{**}(K)| > 0.1$ and $\cos\theta^*(\pi) < 0.85$, where $\theta^{**}(K) = \text{angle}(\boldsymbol{p}_K^{(\phi \text{ rest})}, \boldsymbol{p}_\pi^{(\phi \text{ rest})})$ and $\theta^*(\pi) = \text{angle}(\boldsymbol{p}_\pi^{(D_s \text{ rest})}, \boldsymbol{p}_{D_s}^{(\text{lab})})$. Figure 4 shows the $M(KK\pi)$ distribution for D_s candidates for $p_T(D_s^+) > 3$ GeV. A clear signal is seen at the nominal value of $M(D_s^+)$. A secondary signal also appears at the nominal value of $M(D^+)$, as expected from the decay of D^+ in the same channel. The resulting mass distribution was fitted to the sum of two modified Gaussians, one for each signal peak. The number of reconstructed D_s^+ mesons yielded by the fit was $N(D_s^+) = 680 \pm 79$. The corresponding result for $p_T(D_s^+) > 2$ GeV was $N(D_s^+) = 773 \pm 96$ (distribution not shown).

4.5 Reconstruction of Λ_c^+ baryons

The Λ_c^+ baryons were reconstructed from the decay channel $\Lambda_c^+ \to K^-p\pi^+$ (+c.c.). Due to trigger availability, the Λ_c^+ sample corresponds to an integrated luminosity of 65 pb^{-1}. In each event, two tracks with the same charges and a third track with opposite charge were combined to form the Λ_c^+ candidates. Only tracks with $p_T(\pi) > 0.5$ GeV, $p_T(K) > 0.75$ GeV and $p_T(p) > 1.3$ GeV were considered. The proton momentum in the laboratory frame is typically larger than that of the pion from the decay due to the large difference of their masses. Therefore, of the two tracks with same charges, to the one with larger (smaller) momentum was assigned the proton (pion) mass. The mass of the kaon was assigned to the track with opposite charge. To suppress the combinatorial background the following cuts were applied: $\cos\theta^*(K) > -0.9$ and $\cos\theta^*(p) > -0.25$, where $\theta^*(K,p) = \text{angle}(\boldsymbol{p}_{K,p}^{(\Lambda_c \text{ rest})}, \boldsymbol{p}_{\Lambda_c}^{(\text{lab})})$. Figure 5 shows the $M(pK\pi)$ distribution for Λ_c candidates. The number of reconstructed Λ_c baryons yielded by the fit was $N(\Lambda_c^+) = 630 \pm 250$.

5 Acceptance corrections

The acceptances were calculated using the Rapgap 2.08 [23] Monte Carlo (MC) model and checked with Herwig 6.1 [24]. The Rapgap MC model was interfaced with Heracles 4.6.1 [25] in order to incorporate first-order electroweak corrections. The generated events were then passed through a full simulation of the detector, using GEANT 3.13 [26] and processed and selected with the same programs as used for the data.

Production cross sections were determined using

$$\frac{d\sigma}{dY} = \frac{N(D)}{\mathcal{A} \cdot \mathcal{L} \cdot \mathcal{B} \cdot \Delta Y}$$

where $N(D)$ is the number of reconstructed D hadrons in a bin ΔY, $\mathcal{A}$ is the reconstruction acceptance (which takes into account migrations, efficiencies and QED radiative effects for that bin) and $\mathcal{L}$ is the integrated luminosity. $\mathcal{B}$ is the branching ratio or the product of the branching ratios for the decay channel used in the reconstruction.

6 Charm fragmentation ratios and fractions [2]

6.1 Ratio of neutral to charged D mesons production rates

The ratio of neutral to charged D meson production rates, $R_{u/d}$, is the ratio of the production cross sections for the sum of direct neutral mesons (D^{*0}, D^0) to the sum of direct charged mesons (D^{*+}, D^+). Direct production of D^0 and D^+ means these mesons do not originate from D^{*0} and D^{*+} decays. As all D^{*0}'s decay into D^0, the ratio is given by

$$R_{u/d} = \frac{\sigma^{\rm untag}(D^0)}{\sigma(D^+) + \sigma^{\rm tag}(D^0)}.$$

The ratio of neutral to charged D meson production rates obtained for the kinematic region $1.5 < Q^2 < 1000$ GeV^2, $0.02 < y < 0.7$, $p_T(D, \Lambda_c) > 3.0$ GeV and $|\eta(D, \Lambda_c)| < 1.6$ is

$$R_{u/d} = 1.46 \pm 0.17^{+0.10}_{-0.34}.$$

The measured ratio is consistent with one. The large systematic effect comes mainly from the signal extraction procedure which also affects the other measurements of ratios and fractions.

The measurement is compared with other values obtained at HERA [2,27] and with those from e^+e^- annihilations [28–30] in Figure 6. All measurements agree within experimental uncertainties.

[2] For all charm fragmentation ratios and fractions the distortions from decays of excited D mesons with non-zero orbital momentum were neglected.

6.2 Strangeness suppression factor

The strangeness suppression factor γ_s is the ratio of twice the cross sections for charmed meson containing a strange quark divided by the cross sections for those containing an up or down quark. As all D^{*+} and D^{*0} decay into either a D^+ or a D^0 and all D_s^{*+} decay into a D_s^+, γ_s is the ratio of twice the D_s^+ cross section to the sum of the "equivalent" D^0 and D^+ cross sections. Equivalent cross sections were defined as the the sums of D^0 and D^+ direct cross sections and contributions from D^{*+} and D^{*0} decays. The strangeness suppression factor is then given by

$$\gamma_s = \frac{2\sigma(D_s^+)}{\sigma(D^+) + \sigma^{\rm untag}(D^0) + \sigma^{\rm tag}(D^0) + 2\sigma^{\rm add}(D^{*+})}.$$

where the same production rates for D^{*0} and D^{*+} have been assumed. The strangeness suppression factor obtained for the kinematic region $1.5 < Q^2 < 1000$ GeV^2, $0.02 < y < 0.7$, $p_T(D,\Lambda_c) > 3.0$ GeV and $|\eta(D,\Lambda_c)| < 1.6$ is

$$\gamma_s = 0.265 \pm 0.035^{+0.039}_{-0.048}.$$

The measurement is compared with other values obtained at HERA [2, 27, 31] and with those from e^+e^- annihilations [32] in Figure 6. All measurements agree within experimental uncertainties.

6.3 Fraction of D mesons produced in a vector state

The fraction of D mesons produced in a vector state is given by the ratio of vector charm-meson production cross sections to the sum of vector and direct pseudoscalar charm-meson production cross sections. The fraction for charged charm-mesons is given by

$$P_V^d = \frac{\sigma^{\rm tag}(D^0)/\mathcal{B}_{D^{*+}\to D^0\pi^+} + \sigma^{\rm add}(D^{*+})}{\sigma(D^+) + \sigma^{\rm tag}(D^0) + \sigma^{\rm add}(D^{*+})},$$

where $\mathcal{B}_{D^{*+}\to D^0\pi^+} = 0.677 \pm 0.005$ [34] is the branching ratio of the $D^{*+} \to D^0\pi^+$ decay.

The fraction of D mesons produced in a vector state for the charged and neutral charm-mesons, considering the same production rates for D^{*0} and D^{*+}, is given by

$$P_V = \frac{2\sigma^{\rm tag}(D^0)/\mathcal{B}_{D^{*+}\to D^0\pi^+} + 2\sigma^{\rm add}(D^{*+})}{\sigma(D^+) + \sigma^{\rm untag}(D^0) + \sigma^{\rm tag}(D^0) + 2\sigma^{\rm add}(D^{*+})}.$$

The fractions P_V^d and P_V measured for the kinematic region $1.5 < Q^2 < 1000$ GeV^2, $0.02 < y < 0.7$, $p_T(D,\Lambda_c) > 3.0$ GeV and $|\eta(D,\Lambda_c)| < 1.6$ are, respectively,

$$P_V^d = 0.590 \pm 0.037^{+0.022}_{-0.018},$$

$$P_V = 0.490 \pm 0.032^{+0.071}_{-0.019}.$$

It can be seen from the measured fractions P_V^d and P_V that naive spin counting, which predicts a value of 0.75, does not hold for charm production.

The measurements are compared with other values obtained at HERA [2, 27] and with those from e^+e^- annihilations [28–30] in Figure 6. All measurements agree within experimental uncertainties.

6.4 Charm fragmentation fractions

The fraction of c quarks hadronising into a particular charm hadron, $f(c \to D, \Lambda_c)$, is the ratio of the charmed-hadron production rate to the sum of the production rate of all charm ground states. The strange-charm baryons Ξ_c^+, Ξ_c^0 and Ω_c^0 cross sections should be included in the sum in addition to the measured D mesons and Λ_c baryons. The production rates for these baryons is expected to be much lower than that for Λ_c^+ due to strangeness suppression. The relative rates for these baryons can be estimated from the non-charm sector as in [33]. Assuming equal production of Ξ^+ and Ξ^0 and that the measured non-charmed Ξ^-/Λ and Ω^-/Λ relative rates, $(6.65 \pm 0.28)\%$ and $(0.42 \pm 0.07)\%$, respectively [34], are similar to the charmed ones, the total rate for the charm-strange baryons should be $(14 \pm 5)\%$ of the Λ_c production rate. Also considering the same production rates for D^{*0} and D^{*+}, the sum of the production rates for all charm ground states is

$$\sum_{all} \sigma_{g.s.} = \sigma(D^+) + \sigma^{\rm untag}(D^0) + \sigma^{\rm tag}(D^0) + 2\sigma^{\rm add}(D^{*+}) + \sigma(D_s^+) + \sigma(\Lambda_c^+) \times 1.14.$$

Therefore, under the same assumptions, the charm fragmentation fractions are:

$$f(c \to D^0) = [\sigma^{\rm untag}(D^0) + \sigma^{\rm tag}(D^0) + \sigma^{\rm add}(D^{*+}) \times (1 + \mathcal{B}_{D^{*+}\to D^0\pi^+})] / \sum_{all} \sigma_{g.s.},$$

$$f(c \to D^{*+}) = [\sigma^{\rm tag}(D^0)/\mathcal{B}_{D^{*+}\to D^0\pi^+} + \sigma^{\rm add}(D^{*+})] / \sum_{all} \sigma_{g.s.},$$

$$f(c \to D^+) = [\sigma(D^+) + \sigma^{\rm add}(D^{*+}) \times (1 - \mathcal{B}_{D^{*+}\to D^0\pi^+})] / \sum_{all} \sigma_{g.s.},$$

$$f(c \to D_s^+) = \sigma(D_s^+) / \sum_{all} \sigma_{g.s.},$$

$$f(c \to \Lambda_c^+) = \sigma(\Lambda_c^+) / \sum_{all} \sigma_{g.s.},$$

The measured fragmentation fractions are shown in Table 1.

The measurements are compared with other values obtained at HERA [2, 27, 31] and with those from e^+e^- annihilations [32] in Figure 7. All measurements agree within experimental uncertainties.

7 Cross sections and pQCD comparisons

7.1 Visible cross sections

The overall D^0, D^+, and D_s^+ acceptances after applying the selection criteria described in sections 3 and 4 for $1.5 < Q^2 < 1000$ GeV^2 and $0.02 < y < 0.7$, transverse momenta $p_T(D^0, D^+) > 3\,\text{GeV}$, $p_T(D_s^+) > 2\,\text{GeV}$ and pseudorapidity $|\eta(D)| < 1.6$, calculated with RAPGAP, are $\approx 42\%$, $\approx 26\%$ and $\approx 17\%$, respectively. The total cross sections in the same region are:

$$\sigma(e^\pm p \to e^\pm D^0 X) = 7.35 \pm 0.35(\text{stat.})^{+0.33}_{-0.30}(\text{syst.}) \pm 0.14(\text{br.})\ \text{nb};$$
$$\sigma(e^\pm p \to e^\pm D^+ X) = 2.90 \pm 0.31(\text{stat.})^{+0.07}_{-0.21}(\text{syst.})^{+0.20}_{-0.18}(\text{br.})\ \text{nb},$$

$$\sigma(e^\pm p \to e^\pm D_s^+ X) = 2.99 \pm 0.38(\text{stat.})^{+0.05}_{-0.21}(\text{syst.})^{+0.78}_{-0.51}(\text{br.})\ \text{nb}$$

The main source of systematical uncertainties are the Monte Carlo model used to correct the data and the signal reconstruction. The third set of uncertainties quoted for the measured cross sections are due to the branching-ratio uncertainties[3]

QCD NLO predictions for the measured cross sections of this paper were obtained using the HVQDIS program [35] based on the so-called fixed-flavour-number scheme in which, only light quarks (u, d, s) are included in the initial-state proton as partons whose distributions obey the DGLAP equations [36], and the $c\bar{c}$ is produced via the BGF mechanism [37] with NLO corrections [38]. The inputs used to obtain the predictions for D meson are the following. The ZEUS NLO QCD global fit [39, 40] to structure-function data was used as the parameterisation of the proton PDFs. The charm fragmentation to the particular D meson is carried out using the Peterson function [41]. The hadronisation fractions $f(c \to D)$ used those measured in this paper and the Peterson parameter, ϵ, was set to 0.035 [42].

The predictions from the HVQDIS program are 7.62, 2.81 and 3.37 nb, respectively, in good agreement with the data. The uncertainties on those predictions have been

[3] Contributions from uncertainties of different branching ratios were added in quadrature.

thoroughly studied in [3]. They amount to approximately 15% being dominated by the input PDF and the mass of the charm quark.

The contribution to the cross sections from D mesons produced in $b\bar{b}$ events amounts only to a few percent. The measured cross sections presented here have these contributions already substracted.

7.2 Differential cross-section measurements

The differential D^0, D^+, and D_s^+ cross sections as a function of Q^2, x, $p_T(D)$ and $\eta(D)$ are shown in Figs. 8, 9 and 10[4].

The cross sections in Q^2 and x both fall by about four orders of magnitude in the measured region. The cross-section $d\sigma/dp_T(D)$ falls by two orders of magnitude with increasing $p_T(D)$.

Figs. 8, 9 and 10 show also the corresponding NLO calculations implemented in the HVQDIS program. For all the cross sections the data is well described by the NLO calculation.

8 Extraction of $F_2^{c\bar{c}}$

The open-charm contribution, $F_2^{c\bar{c}}$, to the proton structure-function F_2 can be defined in terms of the inclusive double-differential $c\bar{c}$ cross section in x and Q^2 by

$$\frac{d^2\sigma^{c\bar{c}}(x,Q^2)}{dxdQ^2} = \frac{2\pi\alpha^2}{xQ^4}\{[1+(1-y)^2]F_2^{c\bar{c}}(x,Q^2) - y^2 F_L^{c\bar{c}}(x,Q^2)\}. \tag{1}$$

In this paper, the $c\bar{c}$ cross section is obtained by measuring the D^0, D^+ and D_s^+ production cross sections and employing the measured hadronisation fractions $f(c \to D)$ to derive the total charm cross section. Since only a limited kinematic region is accessible for the measurement of the D mesons, a prescription for extrapolating to the full kinematic phase space is needed.

Since the structure function varies only slowly, it is assumed to be constant within a given Q^2 and y bin. Thus, the measured $F_2^{c\bar{c}}$ in a bin i is given by

$$F_{2,\mathrm{meas}}^{c\bar{c}}(x_i, Q_i^2) = \frac{\sigma_{i,\mathrm{meas}}(ep \to DX)}{\sigma_{i,\mathrm{theo}}(ep \to DX)} F_{2,\mathrm{theo}}^{c\bar{c}}(x_i, Q_i^2), \tag{2}$$

[4] The data cross sections are not corrected for initial or final state QED radiation; this correction was estimated in [3–5] to amount only a few percent.

where σ_i are the cross sections in bin i in the measured region of $p_T(D)$ and $\eta(D)$. The value of $F_{2\ \mathrm{theo}}^{c\bar{c}}$ was calculated from the NLO coefficient functions [39]. The functional form of $F_{2\ \mathrm{theo}}^{c\bar{c}}$ was used to quote the results for $F_2^{c\bar{c}}$ at convenient values of x_i and Q_i^2 close to the centre-of-gravity of the bin. In this calculation, the same parton densities, charm mass ($m_c = 1.35$ GeV), and factorisation and renormalisation scales ($\sqrt{4m_c^2 + Q^2}$) have been used as for the HVQDIS calculation of the differential cross sections. The hadronisation was performed using the Peterson fragmentation function.

Cross sections in the measured D regions and in appropiate (Q^2,y) bins were extrapolated to the full $p_T(D)$ and $\eta(D)$ phase space using HVQDIS. These bins correspond to the Q^2 and x baycenter values where the $F_2^{c\bar{c}}$ measurements are given. For the D^0 and D^+ measurements, typical extrapolation factors are between ≈ 17 at low Q^2 and ≈ 2.5 at high Q^2. For the D_s, the lower p_T requirement bring them down to about 4 and 2 respectively. The beauty contribution was subtracted from the data as in section 7.1. Uncertainties of the extrapolation have been evaluated in [3–5] to be typically smaller than the statistical errors. However, the fact that the data are measured in a small part of the available phase space means that a realistic uncertainty on the extrapolation can not be evaluated. Therefore these extrapolation uncertainties are not included in the systematic uncertainties quoted.

The data are compared in Fig. 11 with the previous measurement [3][5] and with the ZEUS NLO QCD fit [39]. The two sets of data are consistent. The prediction describes the data well for all Q^2 and x. The uncertainty on the theoretical prediction is that from the PDF fit propagated from the experimental uncertainties of the fitted data.

9 Summary

The production of D^0, D^+, D_s^+ and D^{*+} charm mesons and Λ_c^+ charm baryons has been measured in DIS at HERA in the kinematic region $1.5 < Q^2 < 1000$ GeV^2, $0.02 < y < 0.7$, $p_T(D, \Lambda_c^+) > 3.0$ GeV and $|\eta(D, \Lambda_c^+)| < 1.6$ with the ZEUS detector. The ratio of neutral and charged D-meson production rates, the strange suppression factor, the fraction of charged and the sum of charged and neutral charm mesons produced in a vector state and the fractions of c quarks hadronising as D^0, D^+, D_s^+, D^{*+} and Λ_c^+ hadrons were determined in the above kinematic renge. All fragmentation ratios and fractions agree with those obtained in charm production at HERA and in e^+e^- annihilations, confirming the universality of charm fragmentation.

The D^0, D^+ and D_s^+ measured differential cross sections are also used to check the

[5] The "tag" part of our D^0 sample is included in the D^{*+} measurement of [3]

predictions of NLO QCD. The ZEUS NLO PDF, which was fit to recent inclusive DIS data, was used. A good description is observed; this is consistent with a universal gluon density in the proton.

The double-differential cross section in y and Q^2 have been used to extract the open-charm contribution to F_2, by using the NLO QCD calculation to extrapolate outside the measured $p_T(D)$ and $\eta(D)$ regions. The $F_2^{c\bar{c}}$ values obtained from the different D mesons measured are in accord among them and with previous, D^* based, results.

References

[1] For a review see J.C. Collins, D.E. Soper, and G. Sterman, *Perturbative QCD*, A.H. Mueller (ed.) World Scientific, Singapore (1989).

[2] ZEUS Coll., S. Chekanov et al., Eur. Phys. J. **C 44**, 351 (2005).

[3] ZEUS Coll., S. Chekanov et al., Phys. Rev. **D 69**, 012004 (2004).

[4] ZEUS Coll., J. Breitweg et al., Eur. Phys. J. **C 12**, 35 (2000).

[5] ZEUS Coll., J. Breitweg et al., Phys. Lett. **B 407**, 402 (1997).

[6] H1 Coll., A. Aktas et al., Eur. Phys. J. **C 40**, 349 (2005).

[7] H1 Coll., C. Adloff et al., Phys. Lett. **B 528**, 199 (2002).

[8] H1 Coll., C. Adloff et al., Z. Phys. **C 72**, 593 (1996).

[9] H1 Coll., C. Adloff et al., Nucl. Phys. **B 545**, 21 (1999).

[10] ZEUS Coll., J. Breitweg et al., Phys. Lett. **B 481**, 213 (2000).

[11] ZEUS Coll., J. Breitweg et al., Eur. Phys. J. **C 6**, 67 (1999).

[12] ZEUS Coll., J. Breitweg et al., Phys. Lett. **B 401**, 192 (1997).

[13] H1 Coll., A. Aktas et al., Phys. Lett. **B 621**, 56 (2005), hep-ex/0503038.

[14] H1 Coll., S. Aid et al., Nucl. Phys. **B 472**, 32 (1996).

[15] H1 Coll., A. Aktas et al., Eur. Phys. J. **C 38**, 447 (2005).

[16] ZEUS Coll., U. Holm (ed.), *The ZEUS Detector*. Status Report (unpublished), DESY (1993), available on `http://www-zeus.desy.de/bluebook/bluebook.html`.

[17] N. Harnew et al., Nucl. Inst. Meth. **A 279**, 290 (1989);
B. Foster et al., Nucl. Phys. Proc. Suppl. **B 32**, 181 (1993);
B. Foster et al., Nucl. Inst. Meth. **A 338**, 254 (1994).

[18] M. Derrick et al., Nucl. Inst. Meth. **A 309**, 77 (1991);
A. Andresen et al., Nucl. Inst. Meth. **A 309**, 101 (1991);
A. Caldwell et al., Nucl. Inst. Meth. **A 321**, 356 (1992);
A. Bernstein et al., Nucl. Inst. Meth. **A 336**, 23 (1993).

[19] H. Abramowicz, A. Caldwell and R. Sinkus, Nucl. Inst. Meth. **A 365**, 508 (1995).

[20] F. Jacquet and A. Blondel, *Proceedings of the Study for an ep Facility for Europe*, U. Amaldi (ed.), p. 391. Hamburg, Germany (1979). Also in preprint DESY 79/48.

[21] U. Bassler and G. Bernardi, Nucl. Inst. Meth. **A 361**, 197 (1995).

[22] D. Bailey and R. Hall-Wilton, Nucl. Instrum. Meth. **A515**, 37 (2003).

[23] H. Jung, Comp. Phys. Comm. **86**, 147 (1995).

[24] G. Marchesini et al., Preprint Cavendish-HEP-99/17 (hep-ph/9912396), 1999; G. Marchesini et al., Comp. Phys. Comm. **67**, 465 (1992).

[25] A. Kwiatkowski, H. Spiesberger and H.-J. Möhring, Comp. Phys. Comm. **69**, 155 (1992) .

[26] R. Brun et al., GEANT3, Technical Report CERN-DD/EE/84-1, CERN, 1987.

[27] H1 Coll., A. Aktas et al., Eur. Phys. J. **C38**, 447 (2005).

[28] DELPHI Coll., P. Abreu et al., Eur. Phys. J. **C12**, 225 (2000).

[29] ALEPH Coll., R. Barate et al., Eur. Phys. J. **C16**, 597 (2000).

[30] OPAL Coll., K. Ackerstaff et al., Eur. Phys. J. **C5**, 1 (1998).

[31] ZEUS Coll., J. Breitweg et al., Phys. Lett. **B481**, 213 (2000).

[32] L. Gladilin, Preprint hep-ex/9912064, 1999 (1999).

[33] OPAL Coll., G. Alexander et al., Z. Phys. **C72**, 1 (1996).

[34] Particle Data Group, S. Eidelman et al., Phys. Lett. **B592**, 1 (2004).

[35] B.W. Harris and J. Smith, Phys. Rev. **D 57**, 2806 (1998).

[36] V.N. Gribov and L.N. Lipatov, Sov. J. Nucl. Phys. **15**, 438 (1972); L.N. Lipatov, Sov. J. Nucl. Phys. **20**, 94 (1975); G. Altarelli and G. Parisi, Nucl. Phys. **B 126**, 298 (1977); Yu.L. Dokshitzer, Sov. Phys. JETP **46**, 641 (1977).

[37] B.W. Harris and J. Smith, Nucl. Phys. **B 452**, 109 (1995); B.W. Harris and J. Smith, Phys. Lett. **B 353**, 535 (1995). Erratum, Phys. Lett. **B 359**, (1995) 423.

[38] E. Laenen et al., Nucl. Phys. **B 392**, 162 (1993); E. Laenen et al., Nucl. Phys. **B 392**, 229 (1993).

[39] ZEUS Coll., S. Chekanov et al., Phys. Rev. **D 67**, 012007 (2003).

[40] *Public access to ZEUS 2002 PDFs*, available on `http://www-pnp.physics.ox.ac.uk/~cooper/zeus2002.html`.

[41] C. Peterson et al., Phys. Rev. **D 27**, 105 (1983).

[42] P. Nason and C. Oleari, Nucl. Phys. **B 565**, 245 (2000).

	ZEUS prel. (DIS)
$f(c \to D^0)$	$0.584 \pm 0.039^{+0.024}_{-0.050}$
$f(c \to D^{*\pm})$	$0.190 \pm 0.014^{+0.023}_{-0.009}$
$f(c \to D^{\pm})$	$0.194 \pm 0.020^{+0.023}_{-0.011}$
$f(c \to D_s^{\pm})$	$0.103 \pm 0.013^{+0.012}_{-0.017}$
$f(c \to \Lambda_c^{\pm})$	$0.104 \pm 0.048^{+0.018}_{-0.010}$

Table 1: *The fractions of c quarks hadronising as a particular charm hadron.*

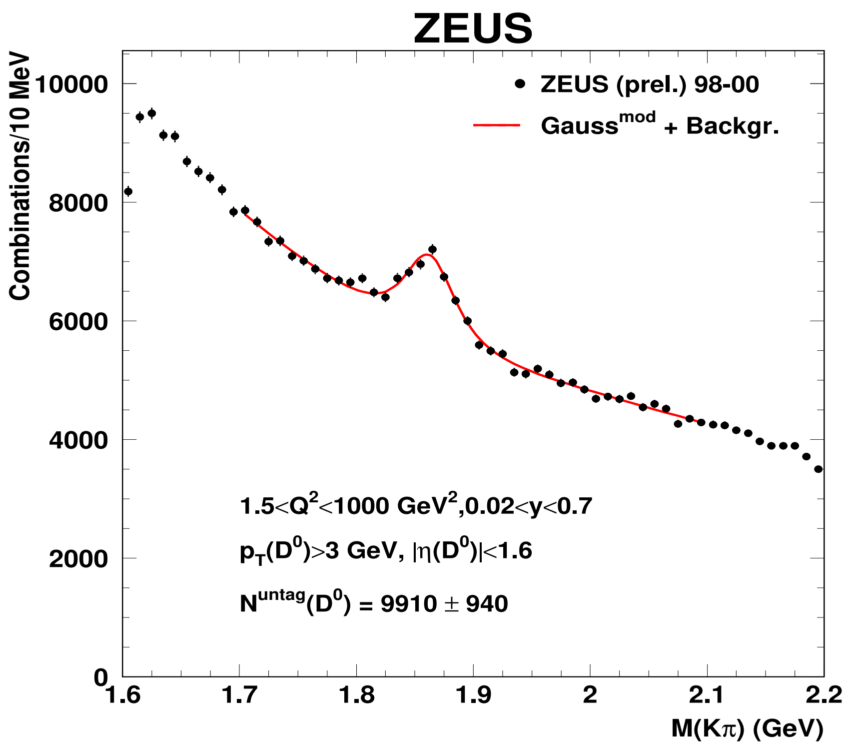

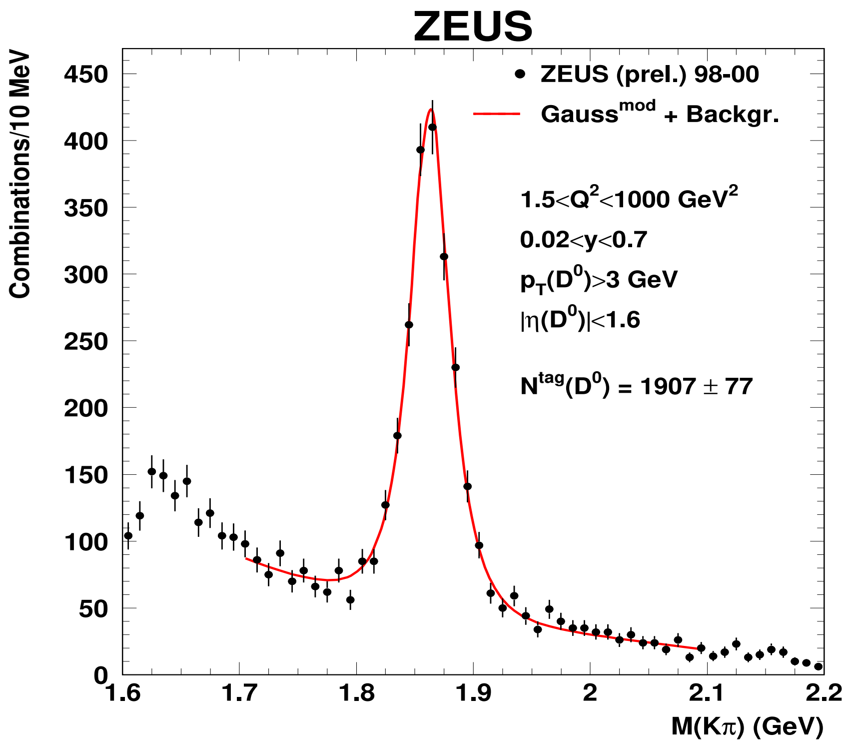

Figure 1: *The $M(K^-\pi^+)$ distribution for the untagged (top) and tagged (bottom) D^0 candidates. The solid curves represent fits to the sum of a modified Gaussian function and a background function of the form $[A + B \cdot M(K\pi)]$ for $M(K\pi) > 1.86\,GeV$ and $[A + B \cdot M(K\pi)] \cdot \exp\{C \cdot [M(K\pi) - 1.86]\}$ for $M(K\pi) < 1.86\,GeV$. The free parameters A, B and C are assumed to be independent for the two $M(K\pi)$ distributions (see [2] for more details).*

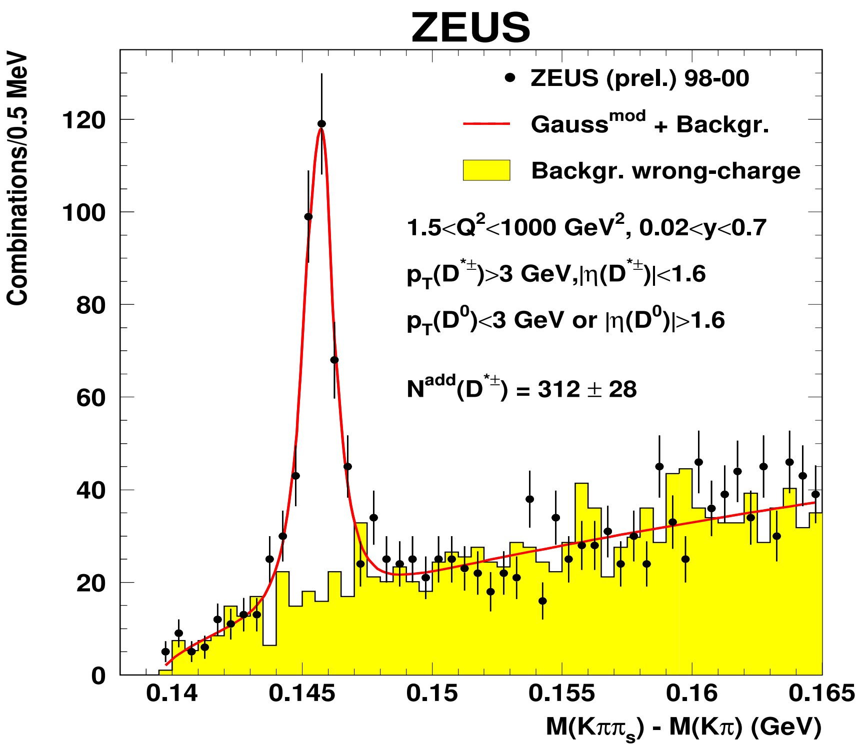

Figure 2: *The distribution of the mass difference* $\Delta M = M(K^-\pi^+\pi_s^+) - M(K^-\pi^+)$ *for additional* D^{*+} *candidates. The histogram shows the* ΔM *distribution for wrong-charge combinations. The solid curve represents a fit to the sum of a modified Gaussian function and a threshold background function, of the form* $A \cdot (\Delta M - m_\pi)^B$*, where* m_π *is the pion mass and* A *and* B *are free parameters.*

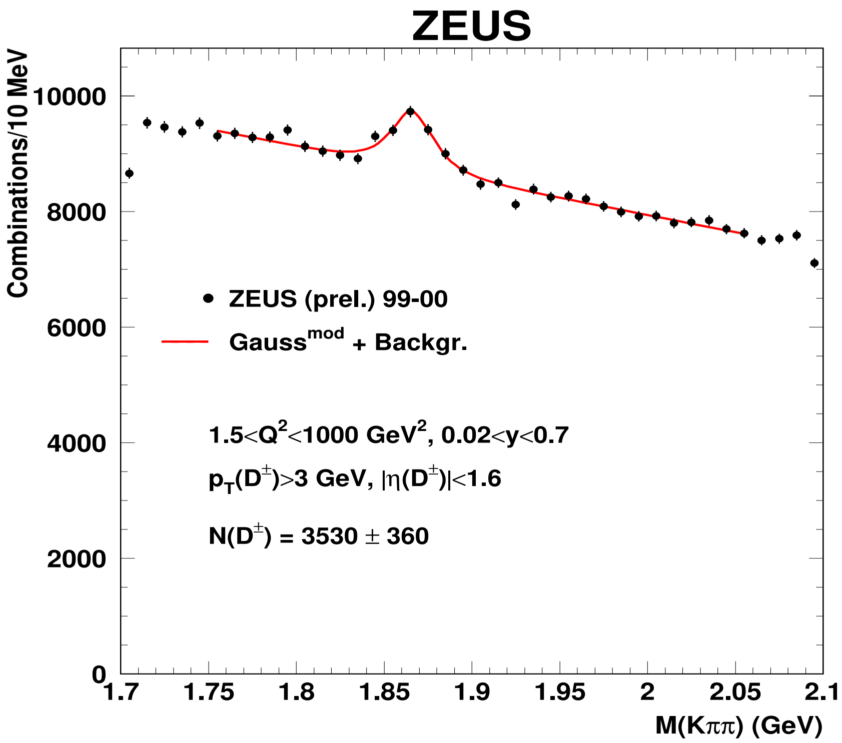

Figure 3: *The $M(K^-\pi^+\pi^+)$ distribution for the D^+ candidates. The solid curve represents a fit to the sum of a modified Gaussian function and a linear background function.*

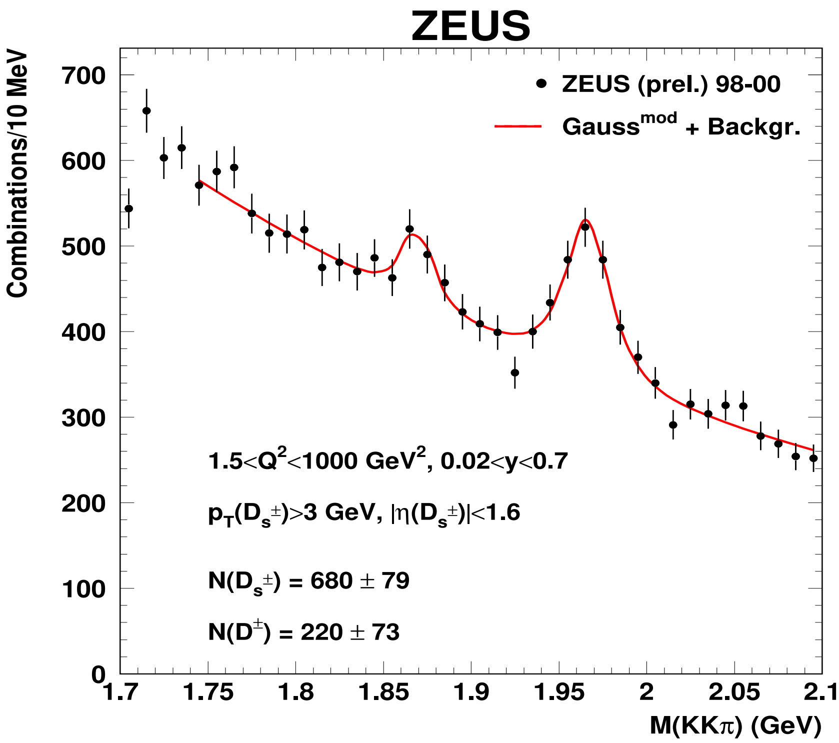

Figure 4: *The $M(K^+K^-\pi^+)$ distribution for the D_s^+ candidates. The solid curve represents a fit to the sum of two modified Gaussian functions and an exponential background function.*

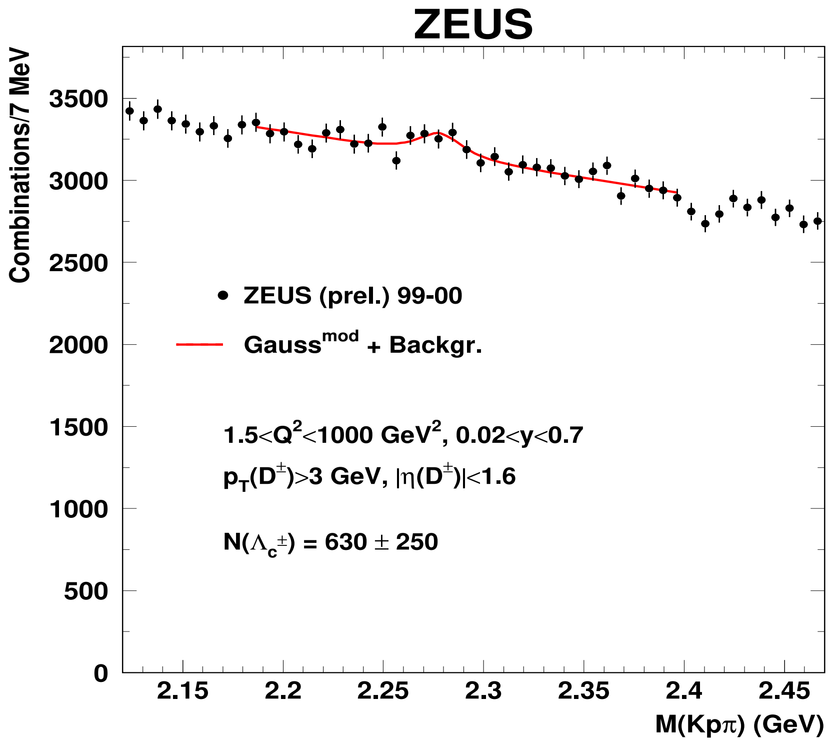

Figure 5: *The $M(pK^-\pi^+)$ distribution for the Λ_c^+ candidates. The solid curve represents a fit to the sum of a modified Gaussian function and a linear background function.*

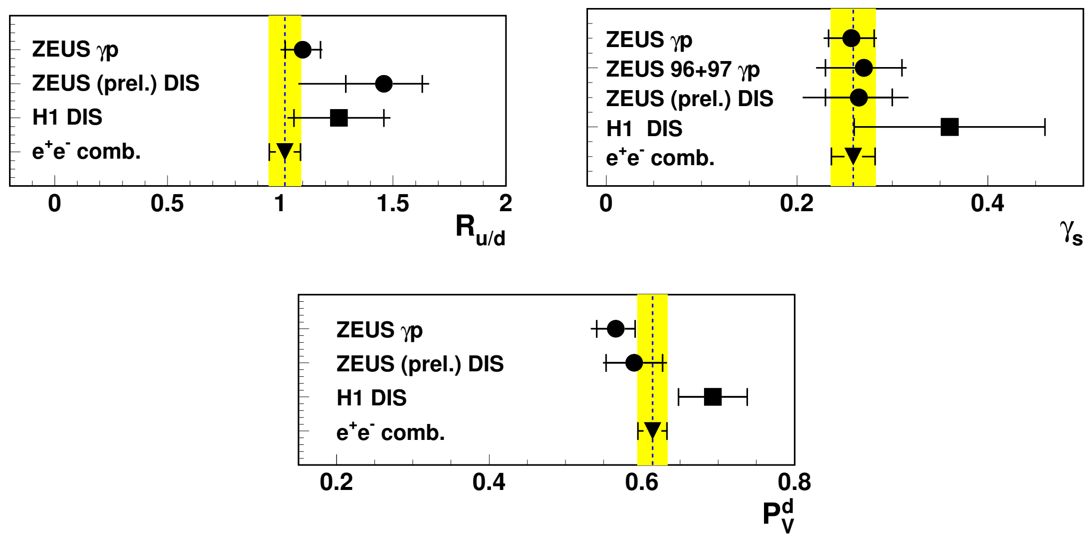

Figure 6: *Comparison of the charm ratios measurements with those obtained in other experiments.*

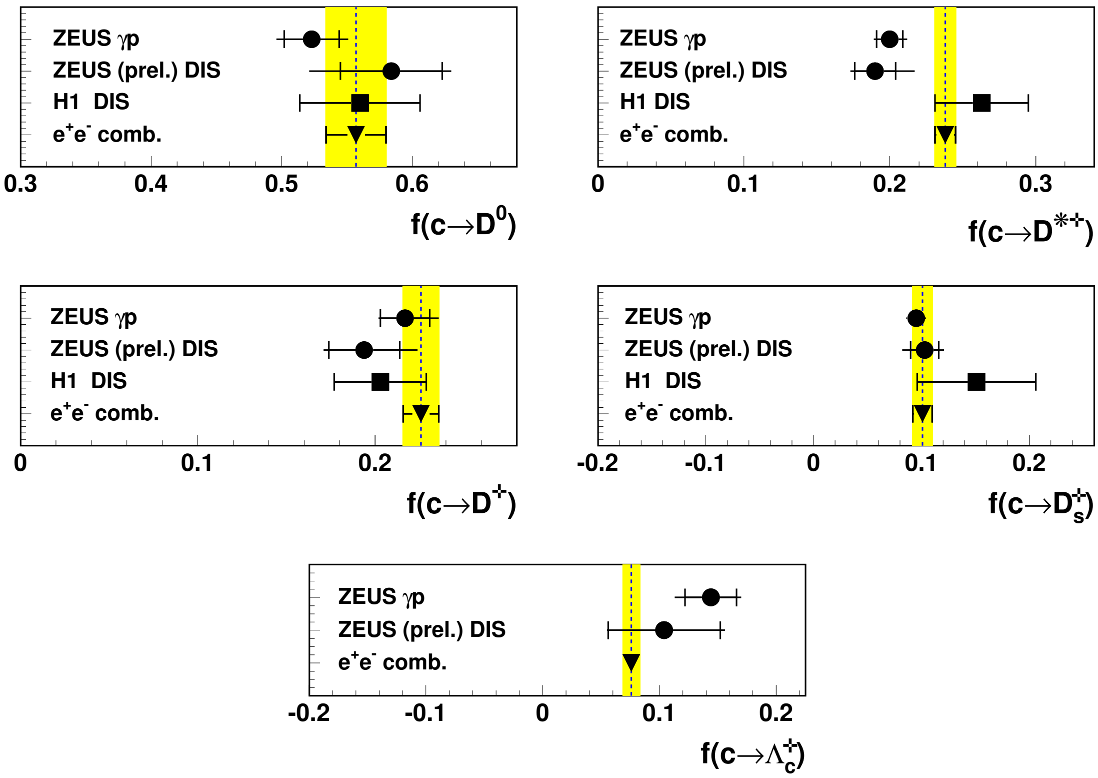

Figure 7: *Comparison of the charm fragmentation fractions measurements with those obtained in other experiments.*

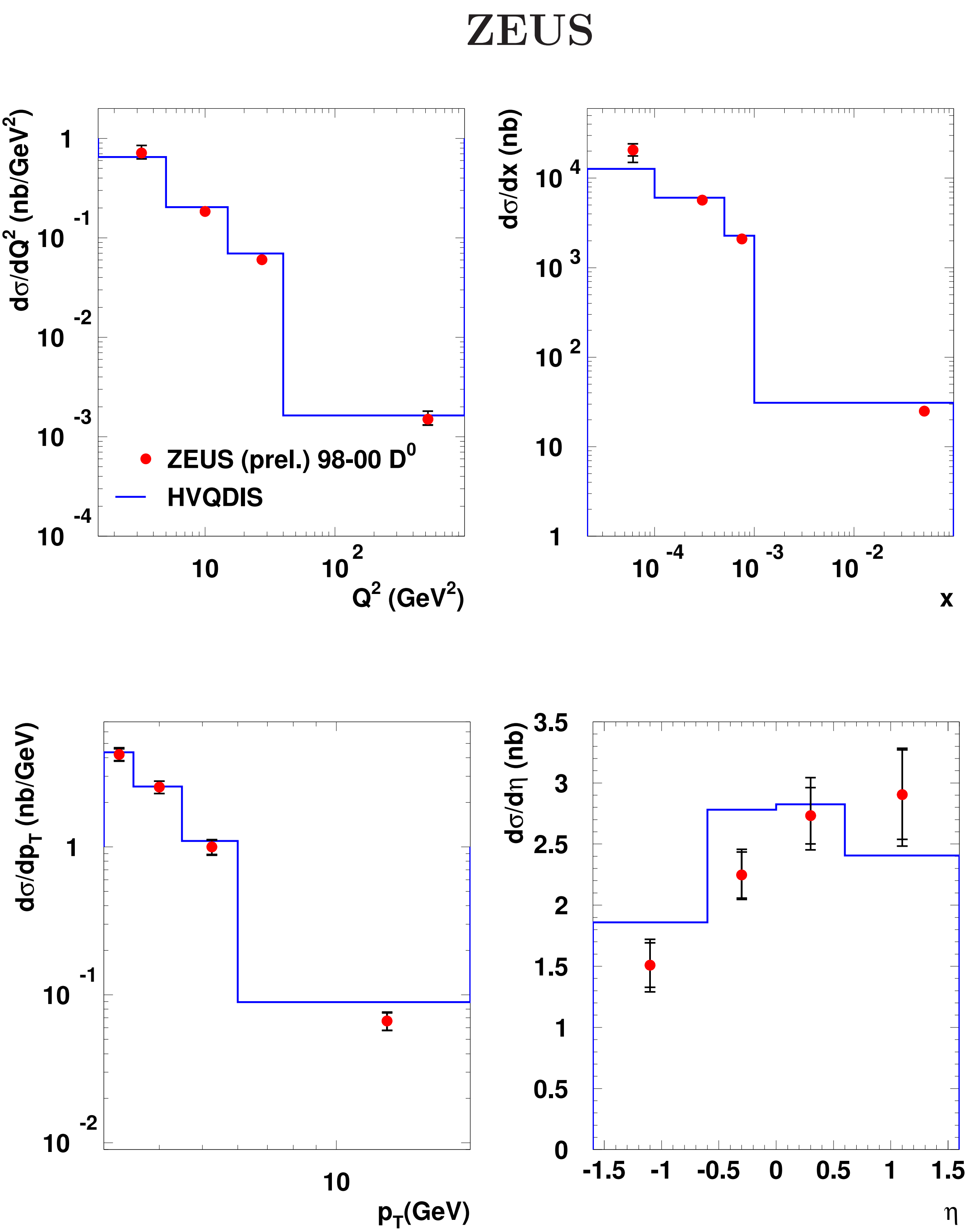

Figure 8: *Differential D^0 cross sections as a function of Q^2, x, $p_T(D^0)$ and $\eta(D^0)$ compared to the NLO QCD calculation of HVQDIS. The inner error bars show the statistical uncertainties and the outer bars show the statistical and systematic uncertainties added in quadrature.*

ZEUS

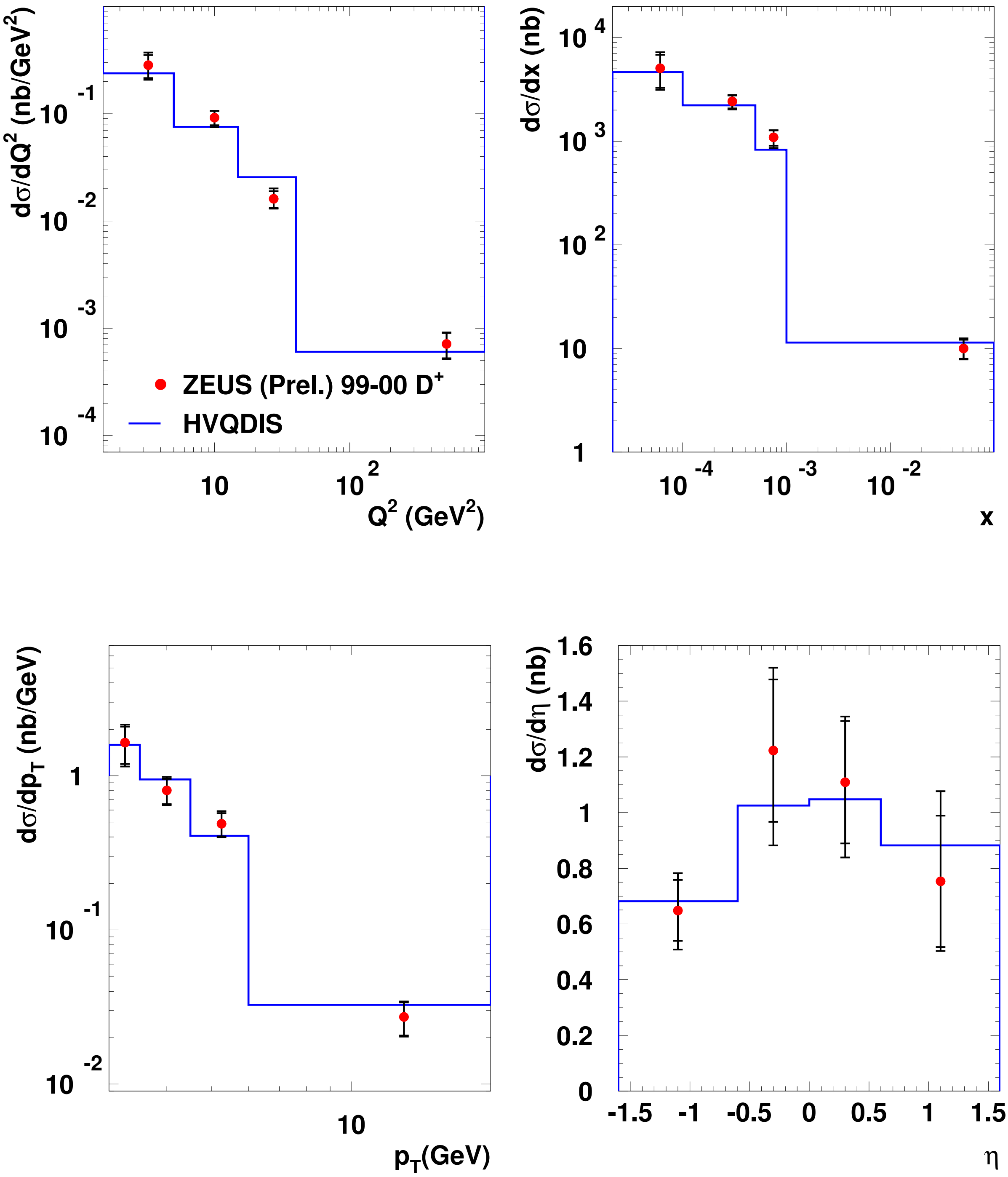

Figure 9: *Differential D^+ cross sections as a function of Q^2, x, $p_T(D^+)$ and $\eta(D^+)$ compared to the NLO QCD calculation of HVQDIS. The inner error bars show the statistical uncertainties and the outer bars show the statistical and systematic uncertainties added in quadrature.*

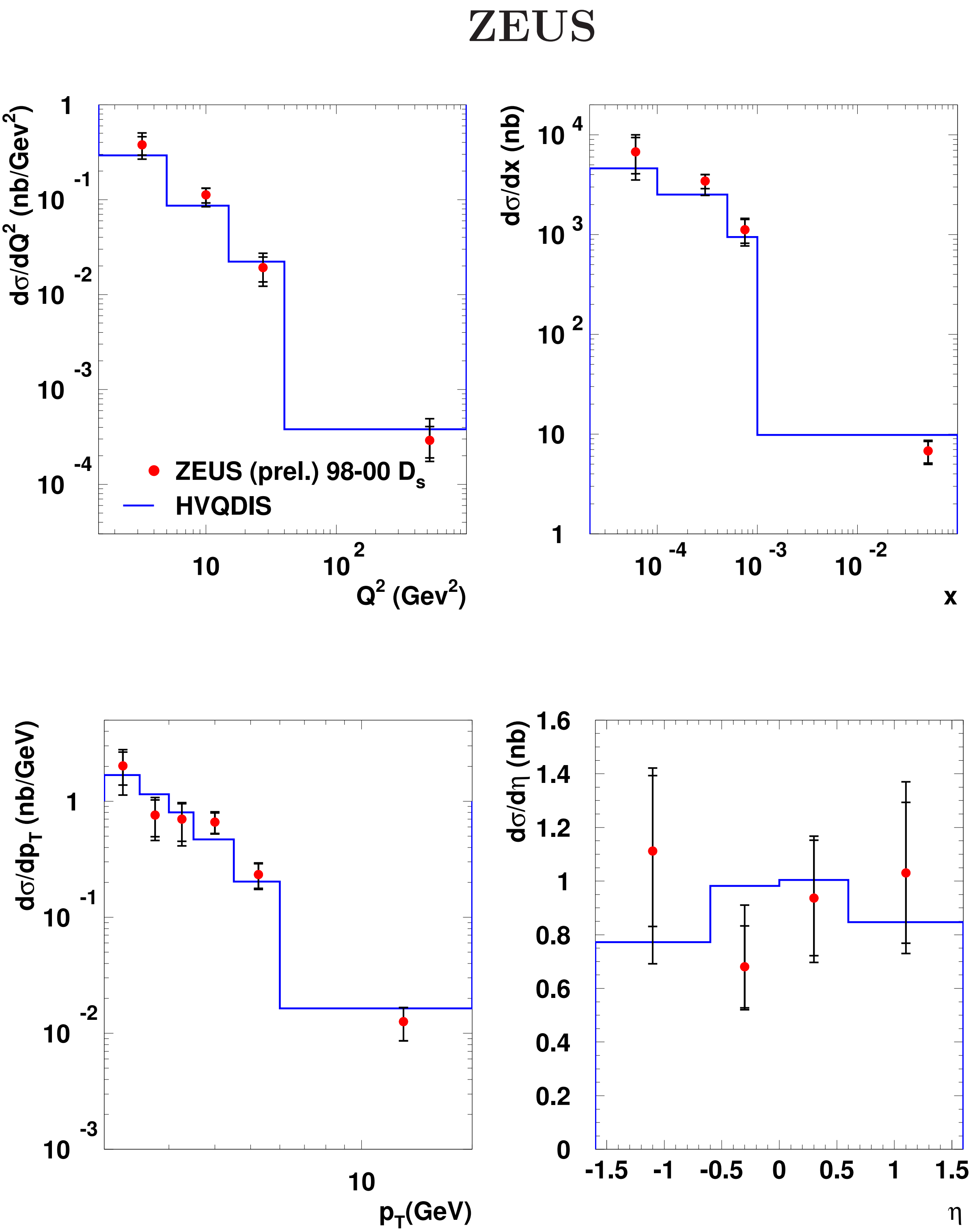

Figure 10: *Differential D_s^+ cross sections as a function of Q^2, x, $p_T(D_s^+)$ and $\eta(D_s^+)$ compared to the NLO QCD calculation of HVQDIS. The inner error bars show the statistical uncertainties and the outer bars show the statistical and systematic uncertainties added in quadrature.*

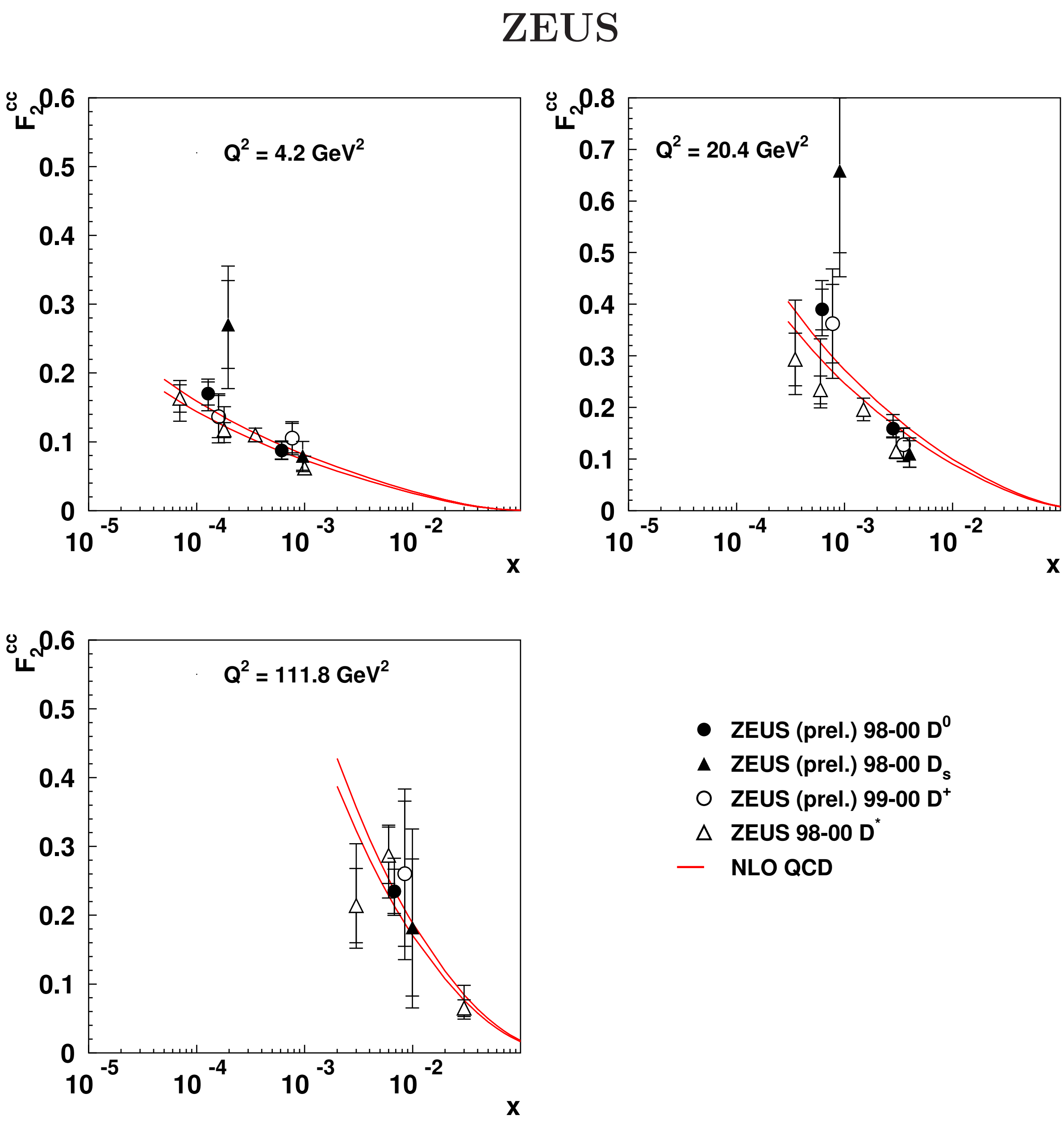

Figure 11: *The measured $F_2^{c\bar{c}}$ at Q^2 values between 2 and 500 GeV^2 as a function of x. The current data are compared with the previous ZEUS measurement [3]. The data are shown with statistical uncertainties (inner bars) and statistical and systematic uncertainties added in quadrature (outer bars). The lower and upper curves show the fit uncertainty propagated from the experimental uncertainties of the fitted data. Note that the "tag" part of the D^0 sample is included in the $D^{*\pm}$ measurement.*